

Supporting Information

to

Restricted Dynamics of a deuterated linker grafted

on SBA-15 revealed by Deuterium MAS NMR

S. Jayanthi^{1†}, M. Werner^{2†}, Y. Xu², G. Buntkowsky^{2*} and S. Vega^{1*}

¹Department of Chemical Physics, Weizmann Institute of Science, Rehovot, Israel – 76100.

² Eduard-Zintl-Institut für Anorganische und Physikalische Chemie, Technische Universität Darmstadt,
Petersenstr. 20, D-64287 Darmstadt, Germany

* Author for correspondence: Gerd.Buntkowsky@chemie.tu-darmstadt.de, Fax no. +49 6151 16-4347
Shimon.Vega@Weizmann.ac.il, Fax no. +972-8-934-4123

Contents

1. SBA-15 characterization : BET-BJH.....	3
2. Proton Integrated Intensity (vs) weight loss	4
3. MD corresponds to T ₃ , data points shown in (-X, -Y).....	5
4. MD conformation with one hydroxyl: (i) CO---HO	6
5. MD calculation with more accessible hydroxyls: (ii) CO---HO	7
6. MD calculation with more accessible hydroxyls: (iii) NH---OH	8
7. MD conformation providing static tensors.....	9

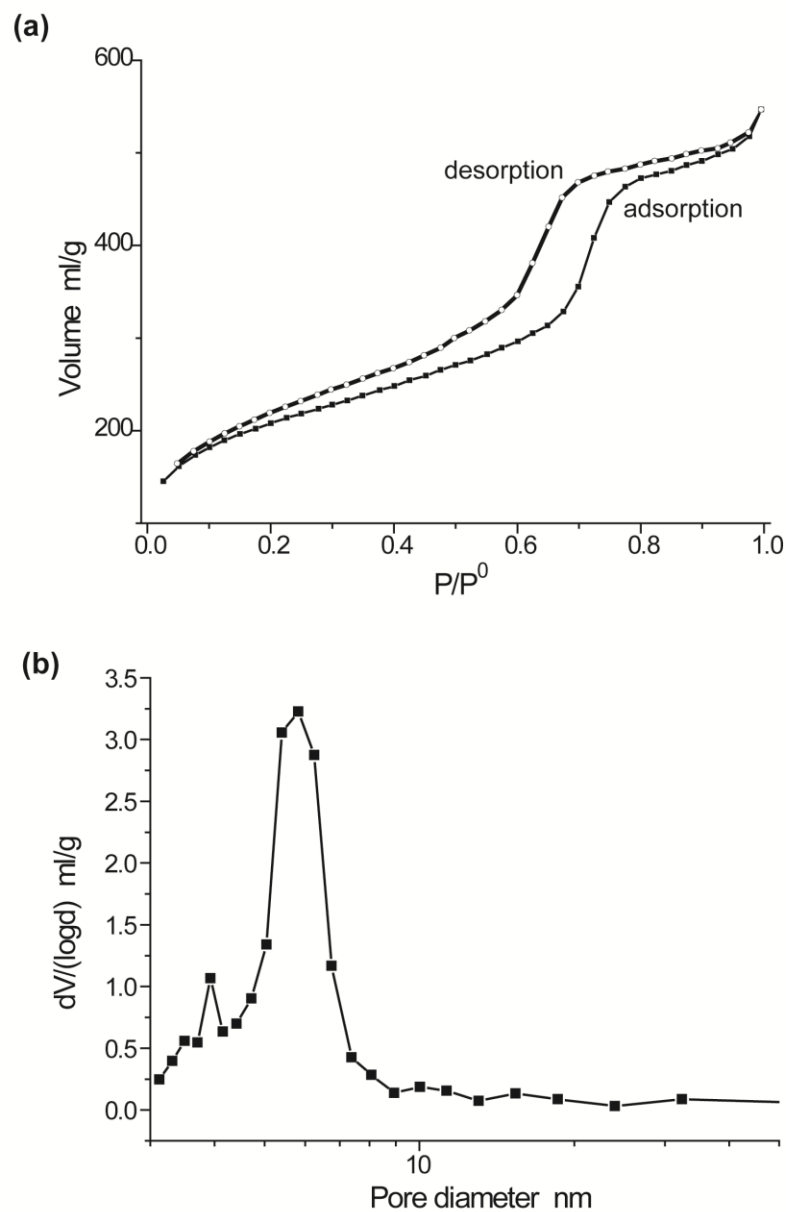


Figure S1: (a) BET adsorption – desorption curve of the synthesized SBA-15. Specific surface area observed is $737 \text{ m}^2/\text{g}$. (b) shows the BJH curve for the same sample. Average pore diameter and pore volume observed are 5.8 nm and 0.81 ml/g .

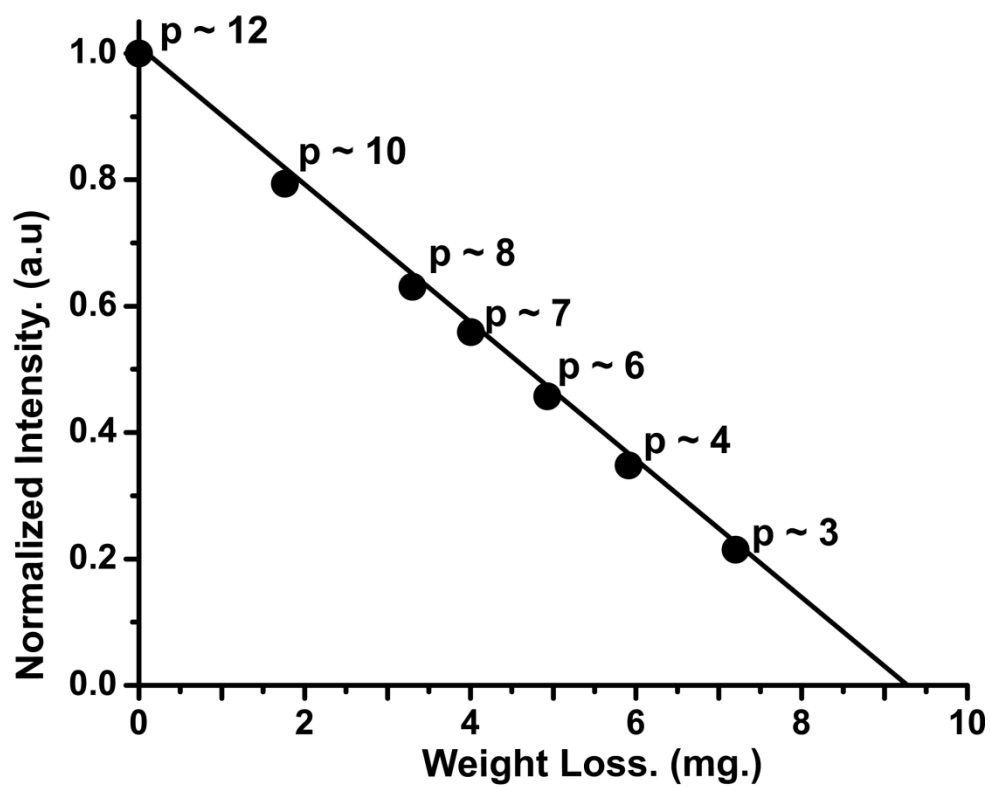


Figure S2: Plot shows the linear variation of integrated intensity of the proton spectra with weight loss of the post grafted sample at various levels of pumping. p values are calculated at each stage and shown therein.

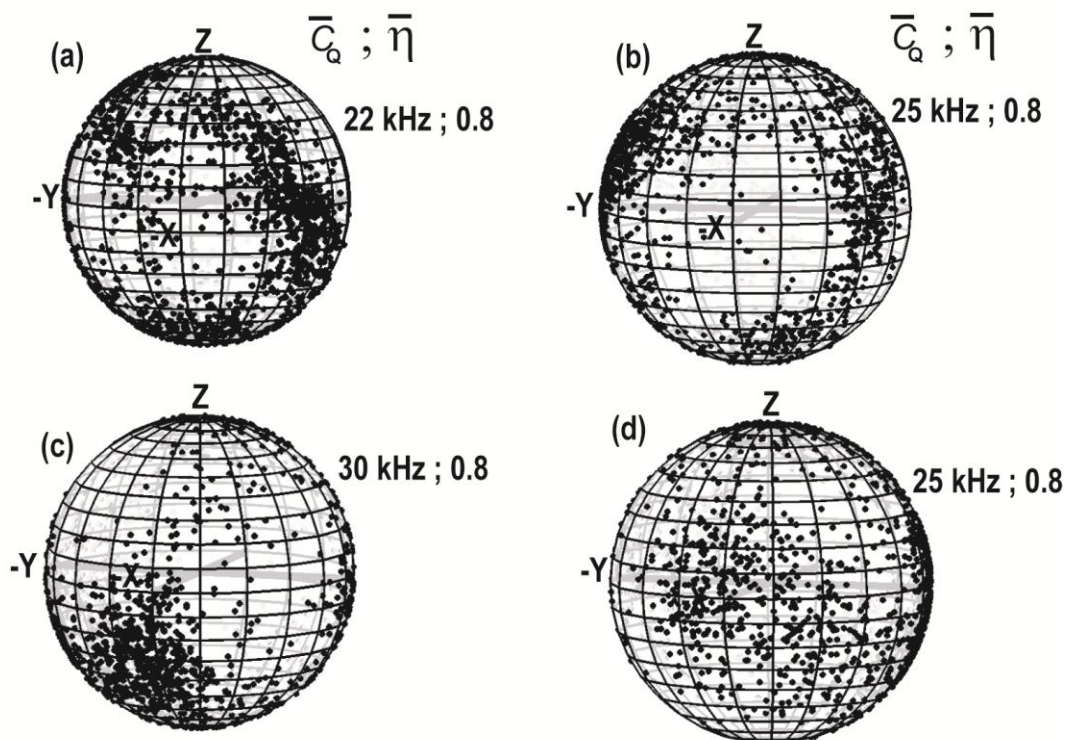


Figure S3: Distribution of the trajectory vectors derived from MD representing the spatial variation of C_1 - $D_{1,2}$ and C_2 - $D_{3,4}$ drawn on a unit sphere are shown in (a,b) and (c,d) respectively. Data points correspond to those behind the sphere shown in Figure 7.

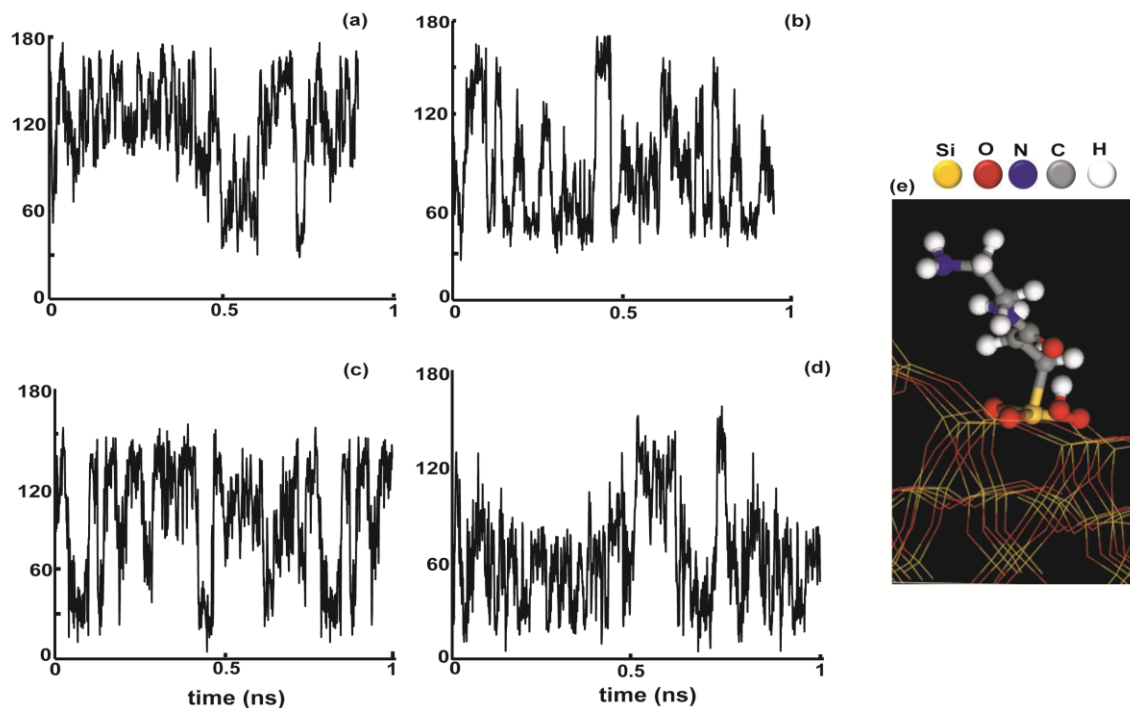


Figure S4: Variation of the time dependent polar angle θ for $C_1-D_{1,2}$ and $C_2-D_{3,4}$ are shown in (a,b) and (c,d) respectively for the model described in Figure 8. The molecular conformation where the mobility of the linker gets restricted through CO---HO hydrogen bonding derived from MD is shown in (e). MD calculation was performed at 295 K for a time period of ~ 1 ns.

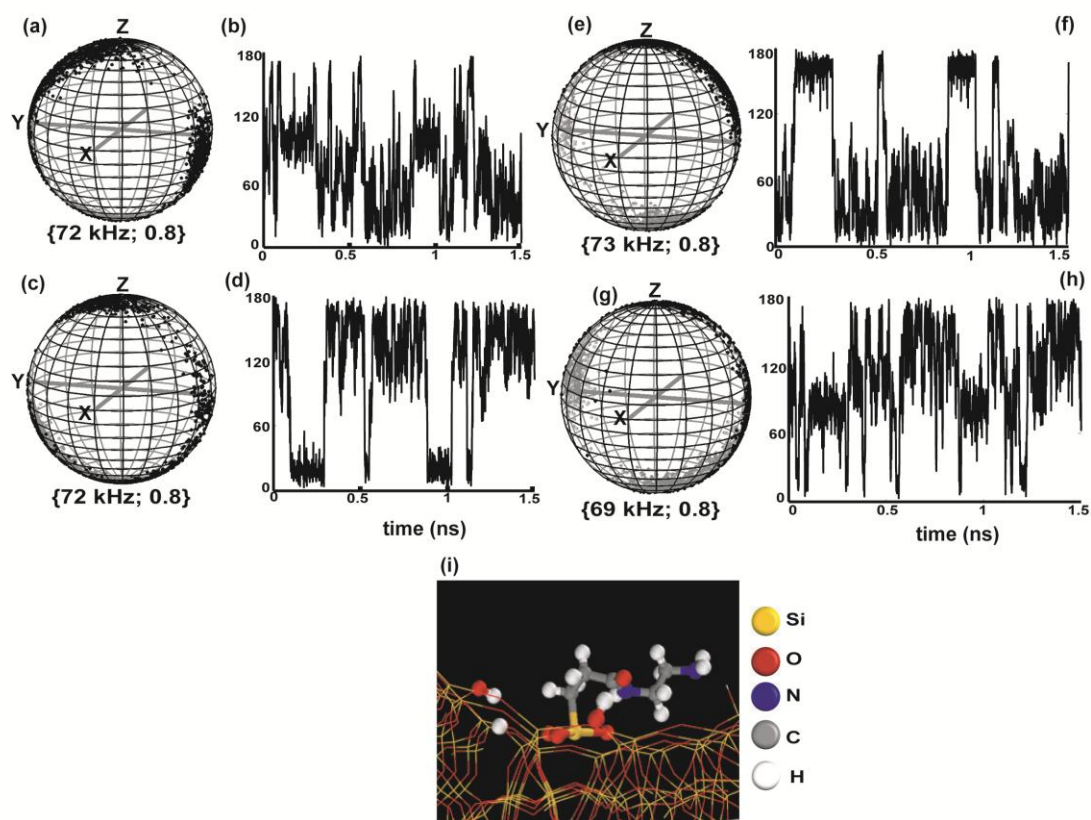


Figure S5: Distribution of the trajectory vectors drawn on a unit sphere along with the variation of the time dependent polar angle θ for C₁-D_{1,2} and C₂-D_{3,4} derived from MD calculation are shown in (a-d) and (e-h) for the model where more than one hydroxyl is introduced. The configuration shown in (i) corresponds to the restricted mobility of the linker through CO---HO hydrogen bonding. MD calculation was performed at 295 K for a time period of ~ 1.5 ns. Averaged quadrupolar parameters calculated are shown therein. Trajectories behind the sphere are drawn in grey.

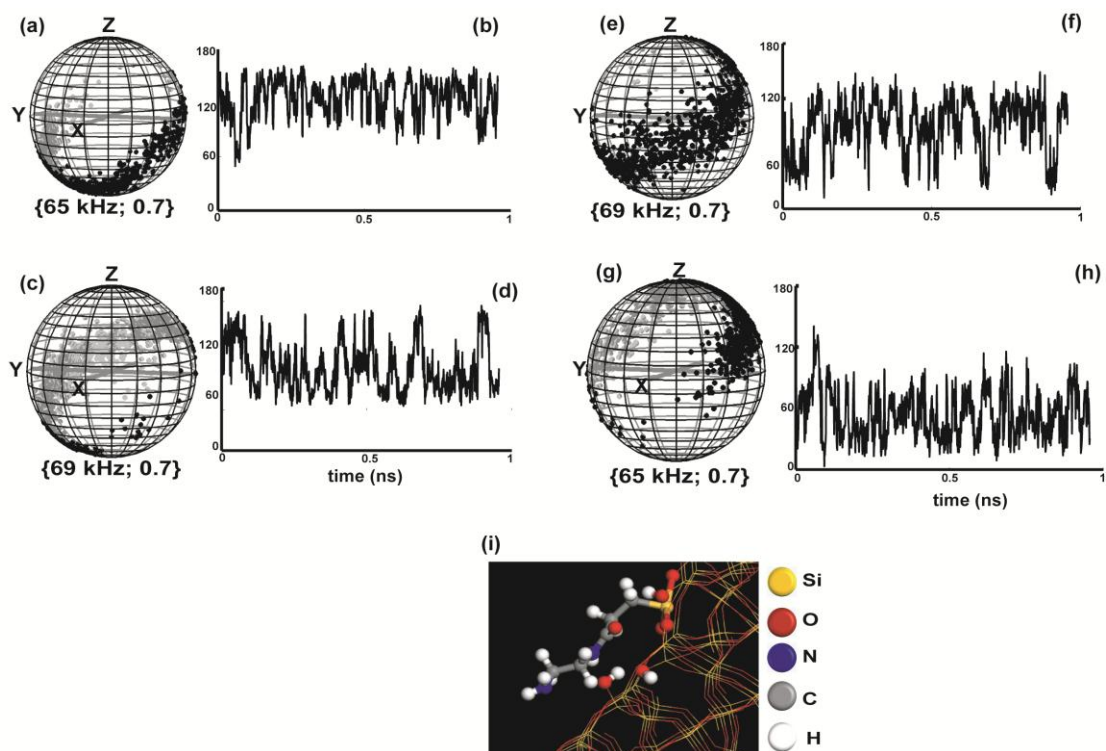


Figure S6: Distribution of the trajectory vectors drawn on a unit sphere along with the variation of the time dependent polar angle θ for $C_1-D_{1,2}$ and $C_2-D_{3,4}$ derived from the MD calculation are shown in (a-d) and (e-h) for the model with more than one hydroxyl on the surface. Molecular conformation where the linker gets bound to the surface hydroxyl through NH---OH hydrogen bonding is shown in (i). MD calculation was performed at 295 K for a time period of ~ 1 ns. Averaged quadrupolar parameters calculated are shown therein. Trajectories behind the sphere are drawn in grey.

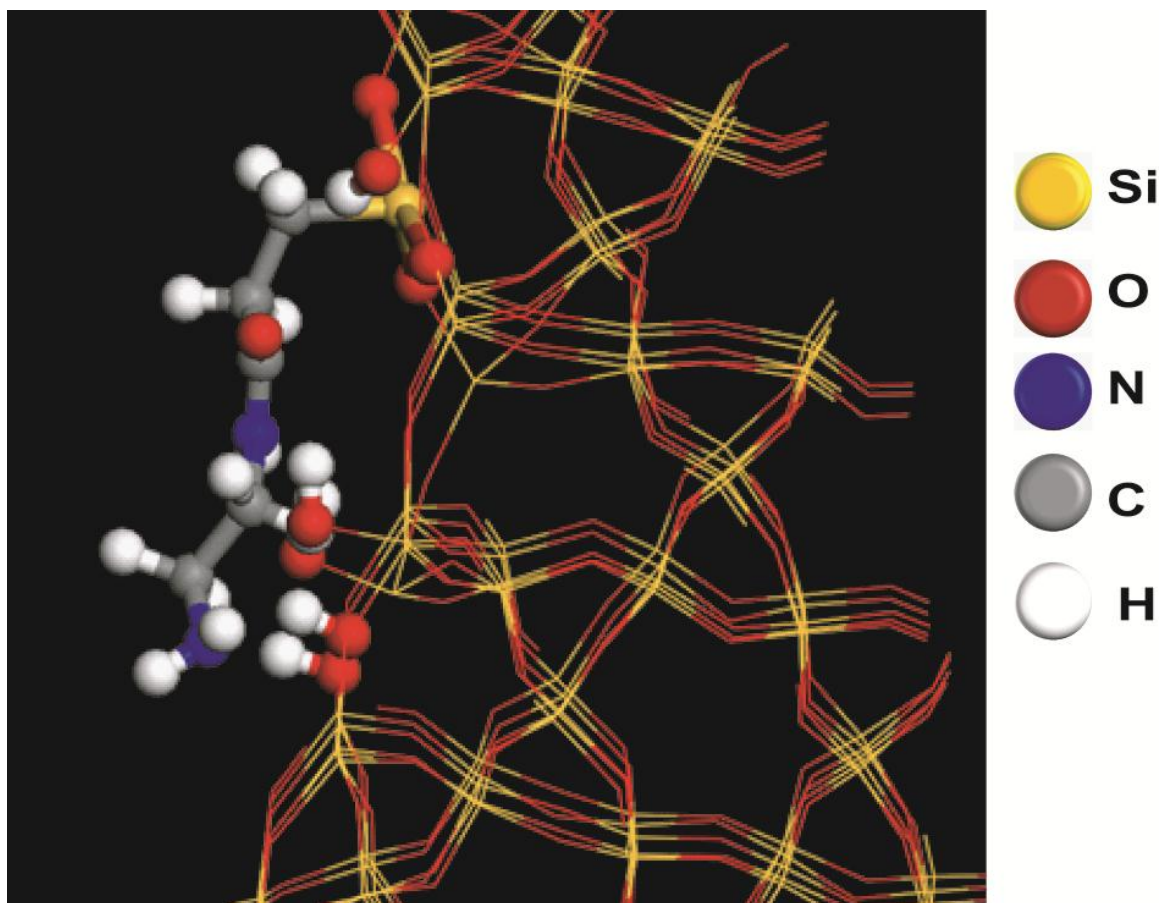


Figure S7: Molecular conformation where the linker gets bound to the surface through NH---OH and NH₂---OH hydrogen bonding thereby resulting in static quadrupolar interaction parameters is shown. MD calculation was performed at 295 K for a time period of ~ 2 ns.